Adsorption and Tautomerization Reaction of Acetone on Acidic Zeolites: The Confinement Effect in Different Types of Zeolites

ARTICLE *in* THE JOURNAL OF PHYSICAL CHEMISTRY C · AUGUST 2010

Impact Factor: 4.77 · DOI: 10.1021/jp1058947

4 AUTHORS, INCLUDING:

Bundet Boekfa
Kasetsart University
25 PUBLICATIONS **330** CITATIONS

SEE PROFILE

Piboon Pantu
Kasetsart University
31 PUBLICATIONS **566** CITATIONS

SEE PROFILE

Adsorption and Tautomerization Reaction of Acetone on Acidic Zeolites: The Confinement Effect in Different Types of Zeolites

Bundet Boekfa,[†,‡,§] Piboon Pantu,[†,‡,§] Michael Probst,[⊥] and Jumras Limtrakul*[,†,‡,§]

Laboratory for Computational and Applied Chemistry, Department of Chemistry, Faculty of Science, Kasetsart University, Bangkok 10900, Thailand, Center of Nanotechnology, Kasetsart University Research and Development Institute, Kasetsart University, Bangkok 10900, Thailand, NANOTEC Center of Nanotechnology, National Nanotechnology Center, Kasetsart University, Bangkok 10900, Thailand, and Institute of Ion Physics and Applied Physics, University of Innsbruck, A-6020 Innsbruck, Austria

Received: June 26, 2010; Revised Manuscript Received: August 4, 2010

The adsorption and tautomerization reaction of acetone in H-FER, H-ZSM-5, and H-MCM-22 zeolites has been studied using full quantum calculations at the M06-2X/6-311+G(2df,2p) level of theory. The combination of a large quantum cluster and this meta-hybrid density functional results in reasonably accurate adsorption energies of −26.9, −28.1, and −23.9 kcal/mol for acetone adsorption in H-FER, H-ZSM-5, and H-MCM-22, respectively. Due to the acidity of the zeolite and the framework confinement effect, the tautomerization of acetone proceeds through a much lower activation barrier than in the isolated gas phase or in the presence of water molecules alone. The activation energies are calculated to be 24.9, 20.5, and 16.6 kcal/mol in H-FER, H-ZSM-5 and H-MCM-22, respectively. The endothermic reaction energy decreases with increasing of the zeolite pore sizes and amounts to 22.7, 17.6, and 15.9 kcal/mol for the reaction in H-FER, H-ZSM-5 and H-MCM-22, respectively. In addition, the adsorbed acetone enol is found to be highly unstable in the zeolite framework and readily reverse-transforms to adsorbed acetone with a very small activation energy. The activity trend and relative stabilities of the adsorbed keto and enol forms are well correlated with the interactions within the Brønsted acid site.

1. Introduction

Aldol condensation is one of the most important C−C bond forming reactions for organic synthesis.[1−3] Aldol condensation of acetone can be readily catalyzed by acidic or basic reagents. In a confined space of microporous zeolites, reactions of acetone over the Brønsted acid site selectively produce mesityl oxide.[4−7] The mesityl oxide can be hydrogenated to produce methyl isobutyl ketone, which is widely used as a solvent for paints, lacquers, and certain types of polymers and resins. The process can be carried out in a single step over bifunctional catalysts (e.g., Pt/H-ZSM-5,[8] Pd/H-MCM-22,[9] etc.). Aldol condensation is very important for the transformation of acetone to methyl isobutyl ketone.[4−6]

Acetone tautomerization to the enol form is an important initial step of aldol condensation and many reactions of acetone.[1−3] The activity of tautomerization dependents on the acidity and the ionic strength of the reaction media. The fundamental steps of the aldol condensation in acidic zeolites are believed to be similar to the reaction in solution.[4−7] The mechanism consists of the acid-catalyzed tautomerization of acetone. Acetone is transformed to an α,β-unsaturated carbonyl compound. A number of theoretical studies on keto−enol tautomerization of acetaldehyde and acetone have been reported.[10−15] Previous theoretical calculations reported that in the gas phase, acetone tautomerization requires a high activation energy of 64.0−69.2 kcal/mol.[11−15] In solvent-assisted systems, the presence of water molecules can greatly reduce the energy barrier by about 20−30 kcal/mol.[12−15] Theoretical results for the tautomerization reaction over a zeolite catalyst have also been reported[15,16] with the synergistic functions of Brønsted acid and Lewis basic sites on H-ZSM-5, drastically reducing the barrier height for the tautomerization of acetaldehyde to 20.2 kcal/mol.[15]

The interaction between the zeolite framework and an adsorbed molecule, which is generally called the confinement effect,[17,18] also plays an important role for the adsorptions and reactions on zeolites.[17−23] Therefore, the details of the interactions between the reactants and the active site in the zeolite's framework and the influence of the topology close to the active site are important to completely understand the reaction mechanism inside zeolite pores. Recently, the role of the zeolite confinement effect on reactions of unsaturated aliphatic, aromatic and heterocyclic compounds has been successfully studied[24] by using full quantum calculations with the new density functional M06-2X.[25−27]

In this work, we study the mechanism of acetone tautomerization and relative stabilities of the keto and enol form in the isolated phase, in the presence of assisting water molecules, and in zeolite-catalyzed environments. Our aim is to investigate the effects of confinement in different zeolite structures on the tautomerization of acetone. Three different zeolites (H-FER, H-ZSM-5, and H-MCM-22) with different dimensions of pores and cavities are selected for this investigation. Sufficiently large clusters are used to represent the zeolite structures, and the full quantum chemical calculations using the M06-2X method are performed to attempt to account for all interactions between

* Corresponding author. Phone: +66-2-562-5555 ext 2159. E-mail: jumras.l@ku.ac.th.
† Department of Chemistry, Kasetsart University.
‡ Kasetsart University Research and Development Institute, Kasetsart University.
§ National Nanotechnology Center, Kasetsart University.
⊥ Institute of Ion Physics and Applied Physics, University of Innsbruck.

10.1021/jp1058947
Published on Web 08/19/2010

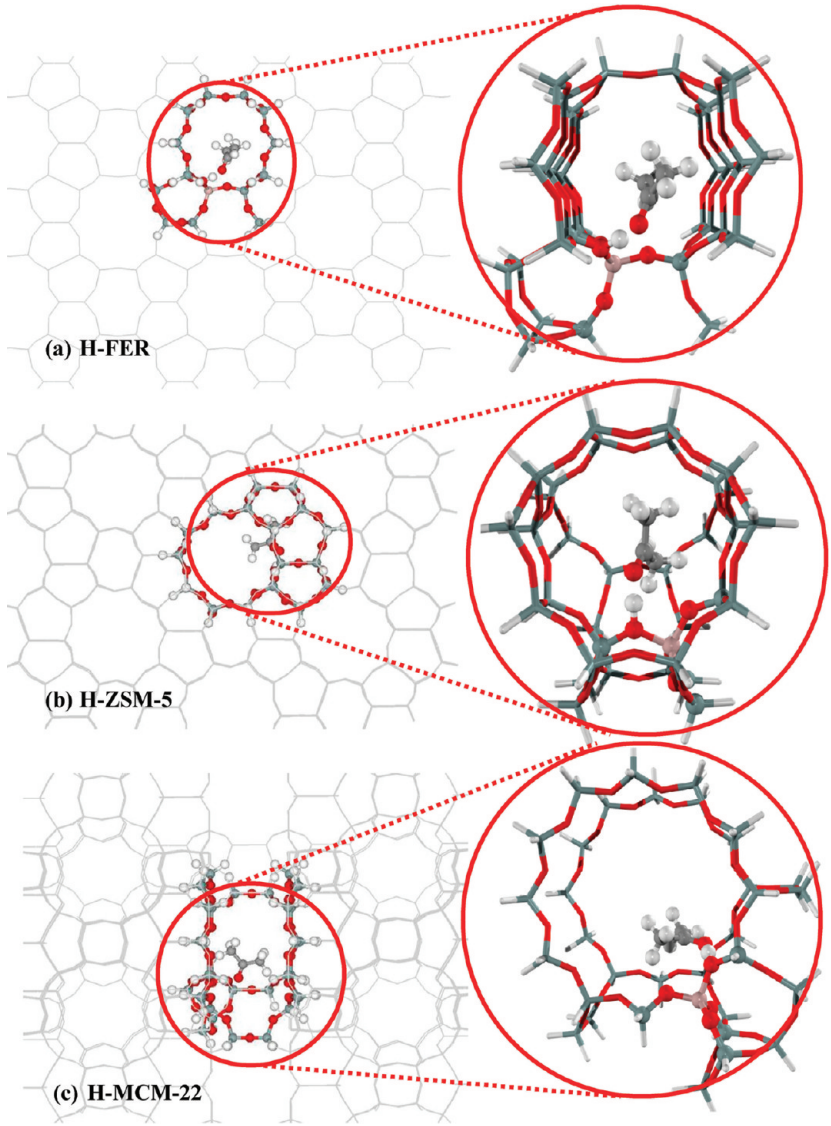

Figure 1. Optimized structures of acetone adsorbed on the 34T model of (a) H-FER, (b) H-ZSM-5, and (c) H-MCM-22 zeolites.

the reactive intermediates and the zeolite acid site and surrounding pore walls.

2. Methodology

34T clusters were taken from crystallographic data of H-FER, H-ZSM-5, and H-MCM-22 zeolites.[28−30] The cluster model of H-FER zeolite covers the 10-membered ring main channel (4.2 × 5.4 Å) that is intersected with the 8-membered ring channel (3.5 × 4.8 Å), as shown in Figure 1a. One silicon atom at the T2 site[31] is replaced with an aluminum atom to represent the Brønsted acid site. The model of H-ZSM-5 represents the intersection cavity where the straight channel (5.4 × 5.6 Å) and the zigzag channel cross (5.1 × 5.4 Å), as shown in Figure 1b. A silicon atom was substituted with an aluminum atom at the most favorable position (T12).[32] The cluster model of H-MCM-22 represents the 12-membered ring channels of the supercage (7.1 × 7.1 × 18.4 Å), as shown in Figure 1c. The substituted aluminum atom is located at the T1 site.[33]

The M06-2X density functional is used in all calculations. During geometry optimizations, only the 5T active region of ≡SiOHAl(OSi)$_2$OSi≡ and the reacting molecule are allowed to relax, while the rest of the structure is kept fixed at the crystallographic coordinates. We also study the reaction of an isolated acetone molecule and the reaction in the presence of water molecules. For geometry optimizations, the 6-31G(d,p) basis set was used. To obtain more accurate interaction energies, single-point calculations with the 6-311+G(2df,2p) basis set were carried out. Transition states were located with the Berny algorithm[34,35] and were checked to confirm that they had one imaginary frequency corresponding to the reaction coordinate. We did not include the zero-point vibrational contributions (ZPVE) to the energies, since the systems are too large to calculate the matrix of second energy derivatives with the M06-2X functional in reasonable time. We are also not aware that this has been performed on systems of similar size. Curtis et al. have performed a study on ethane absorbed on small 3T and 5T clusters.[36,37] They found close agreement between results from G2(MP2) (including ZPVE) and MP2/6-31G(d,p) calculations not including ZPVE, due to cancellation of various effects. We assume that also in our work, the relative changes caused by inclusion of the ZPVE are less than the errors inherent in the functional and basis set. All calculations were performed with the Gaussian 03 code[38] modified to incorporate the Minnesota Density Functionals module 3.1 by Zhao and Truhlar.

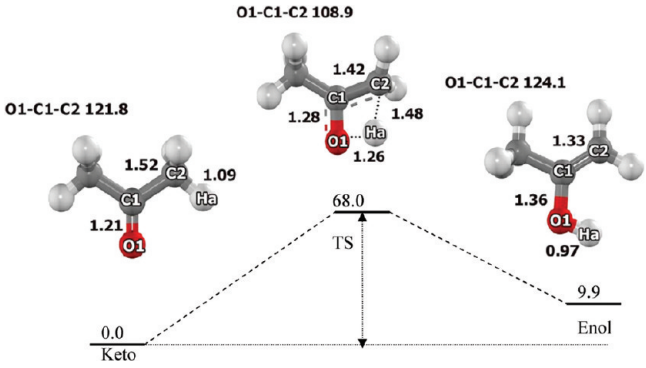

Figure 2. Molecular structures and energy profile of the tautomerization of acetone in an uncatalyzed gas phase environment (M06-2X/6-311+G(2df,2p)//M06-2X/6-31G(d,p) calculations). Distances and energies are given in Å and kcal/mol.

3. Results and Discussion

3.1. Tautomerization of Acetone in the Gas Phase. The uncatalyzed tautomerization of acetone has been extensively studied and was found to occur via a concerted mechanism.[11−15] In this study, we therefore examine the concerted tautomerization mechanism of acetone to validate the applicability of the new density functional M06-2X. Figure 2 shows the potential energy profile and the geometries of acetone, the transition state, and the enol product computed at the M06-2X/6-311+G(2df,2p)//M06-2X/6-31G(d,p) level of theory. At the transition state, the intramolecular proton transfer from the methyl group to the carbonyl oxygen atom takes place. The C2−Ha bond distance increases to 1.48 Å and the O1−Ha decreases to 1.26 Å. At the same time, the C1−O1 carbonyl bond increases from 1.21 to 1.28 Å and the C1−C2 bond length decreases from 1.52 to 1.42 Å. The activation energy is calculated to be 68.0 kcal/mol, and the reaction energy is 9.9 kcal/mol. The computed activation energy and reaction energy agree well with previous theoretical studies that employed the Møller−Plesset perturbation theory.[12,14] In those studies, the activation energies were found to be 64.0 and 69.2 kcal/mol, and the reaction energies were 11.6 and 13.1 kcal/mol. The reaction energies computed in this study are also in reasonable agreement with the experimental results of 12 ± 2 kcal/mol.[39,40]

3.2. Tautomerization of Acetone in Aqueous Solution. For aqueous solutions, it has previously been reported that water molecules can reduce the energy barrier by stabilizing the transition state with hydrogen bonds.[11−15] The tautomerization reaction occurs via cyclic proton transfer networks with water molecules acting as proton donors and acceptors facilitating the reaction. The optimized geometries and energy profiles are presented in Figure 3. The reaction is considered to proceed via the concerted mechanism similar to the reaction in the isolated gas phase. In the presence of a water molecule, acetone interacts with the water molecule by forming 2 hydrogen bonds. Then two protons are transferred simultaneously through the hydrogen bonding network. With two and three additional water molecules, stronger and larger hydrogen bonding networks are formed, as indicated by shorter hydrogen bond distances and angles that are closer to the linear angles of the hydrogen bonds (O···H···O). The addition of water molecules results in a significant reduction of activation energy. The computed activation energies at the M06-2X/6-311+G(2df,2p)//M06-2X/6-31G(d,p) level of theory are 40.2, 32.7, and 33.6 kcal/mol and the reaction energies are 9.7, 7.8, and 8.2 kcal/mol, for the presence of 1, 2, and 3 water molecules, respectively. These results agree well with a previous theoretical study[14] at the MP2/cc-pVTZ//MP2/6-31G(d,p) level, which included the zero-point vibrational energy correction and reported activation energies of 37.5, 30.4, and 29.1 kcal/mol for the presence of 1, 2, and 3 water molecules, respectively. The computed reaction energies in the presence of water molecules were reported to be similar to the reaction energy in the gas phase. The measured reaction enthalpy in aqueous solution was reported as 10.3 ± 0.4 kcal/mol,[41] very close to the gas phase value. Therefore, we conclude that the M06-2X method can give reasonably accurate results for the activation energy and reaction energy of acetone tautomerization as compared with the high level of calculations.

3.3. Tautomerization of Acetone in Zeolites. ***3.3.1. Structure of the Zeolites.*** In this study, we examine the tautomerization of acetone in three different zeolites.[25−27] These three zeolites can be synthesized with a high Si/Al ratio. Therefore, for the sake of model simplicity, we use a single Brønsted acid as an active site for these high silica zeolites. The Brønsted acid is placed on the favorable sites predicted by previous theoretical studies.[31−33] H-FER zeolite has a two-dimensional pore structure with a main straight channel and a smaller channel. The two channels are perpendicular and intersected. In the model used in this study, the Brønsted acid is located at the most favorable position (T2)[31] at the intersection of the 10T main channel (4.2 × 5.4 Å in diameter) and the 8T channel (3.5 × 4.8 Å in diameter) (see Figure 1a). The O1−Hz bond leans toward the middle of the small 8T channel with an angle of about 30° to the axial direction of the 10T main channel.

H-ZSM-5 zeolite is a three-dimensional pore zeolite. The Brønsted acid is located at the T12 position[32] on the window of the zigzag channel that is connected to the intersection cavity. The employed model represents the intersection cavity of ∼9 Å in diameter where the straight channel (10-membered ring, 5.4 × 5.6 Å in diameter) and the zigzag channel (10-membered ring, 5.1 × 5.4 Å in diameter) intersect (see Figure 1b).

H-MCM-22 is also a three-dimensional pore zeolite. The main straight channel is a 10-membered ring having dimensions of 4.0 × 5.5 Å in diameter. It opens to a large cavity called the supercage (7.1 × 7.1 × 18.4 Å). In this study, we consider the acid site to be located on the 12-membered ring in the supercages.

Despite different pore structures, the O1−Hz Brønsted acid bond distance is approximately the same at 0.97 Å in all three zeolite models. The Al···Hz distances are in the range of 2.30−2.43 Å, which compared well with the experimental values of 2.38−2.48 ± 0.04 Å.[42,43]

3.3.2. Acetone Adsorption on H-FER, H-ZSM-5 and H-MCM-22. The optimized structures of acetone adsorbed on the three zeolites are shown in Figure 1, and selected geometric parameters are given in Table 1. In H-FER, an acetone molecule forms a hydrogen bond between its carbonyl oxygen (O3) and the Brønsted acidic proton (Hz). The adsorbed acetone molecule is located in the 10T main channel. The O1−Hz−O3 hydrogen bond angle is 165.8°. This deviation from the linear hydrogen bond angle is due to the alignment of the Brønsted O−H that initially leans toward the small 8T window. The adsorption energy is computed to be −26.9 kcal/mol. In the H-ZSM-5 zeolite, the acetone molecule adsorbs by forming a strong hydrogen bond with the Brønsted acid site. The O1−Hz−O3 bond angle (177.6°) is close to linear, and the adsorption energy is computed to be −28.1 kcal/mol. This value agrees reasonably with an experimental report of the adsorption energy of acetone in H-ZSM-5 of −31.1 kcal/mol.[44] In the large cavity of H-MCM-22, acetone also forms a strong hydrogen bond with the Brønsted acid site on the 12T-membered ring of the

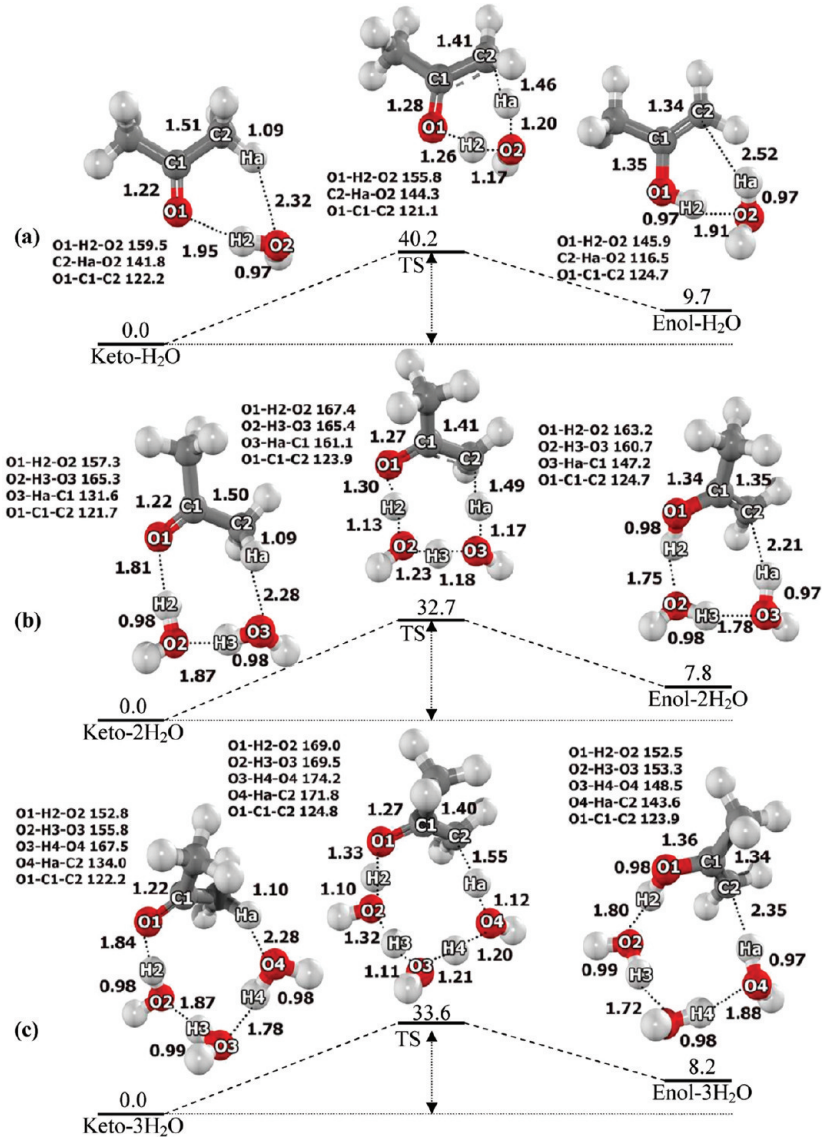

Figure 3. Energy profile and complex geometries in the water-assisted tautomerization of acetone from M06-2X/6-311+G(2df,2p)//M06-2X/6-31G(d,p) calculations: (a) one, (b) two, and (c) three water molecules.

supercage. The O1−Hz−O3 bond angle (171.7°) is also close to linear. The adsorption energy is −23.9 kcal/mol.

The computed adsorption energy is found to be dependent on the pore dimension and also on the local geometry of the Brønsted acid site. H-FER is a medium-pore zeolite with a smaller pore dimension as compared with H-ZSM-5, but the geometry of the Brønsted acid site is not suitable for the adsorption of the acetone molecule. Initially, the acid site bond points toward the small 8T window that is too small to accommodate an acetone molecule. The adsorbed acetone molecule has to be located in the 10T main channel. Therefore, the O1−Hz−O3 hydrogen bond angle deviates from linearity. As a result, the interaction of acetone with the Brønsted acid site in H-FER is not as strong as in H-ZSM-5. The adsorption energy in the medium pore H-ZSM-5 is higher than the large pore H-MCM-22 mainly due to the pore confinement effect.

In our previous work,[20] we demonstrated that in studies of the adsorption of carbonyl compounds in zeolites both van der Waals and electrostatic interactions have to be carefully accounted for. We were able to calculate the adsorption energies of acetaldehyde and acetone in H-ZSM-5 by using the embedded ONIOM(B3LYP:UFF) method. With small cluster models, the computed adsorption energy is underestimated by as much as 16 kcal/mol. In the embedded ONIOM(B3LYP:UFF) method, the UFF force field was used to explicitly account for the short-range van der Waals interactions with the surrounding pore walls, and the embedded Madelung potential was used to account for the long-range electrostatic interactions with the zeolite framework. It has been demonstrated that the short-range van der Waals interactions and the long-range electrostatic interactions with the zeolite framework are both very important to the stabilization of the adsorbed carbonyl compounds in zeolite.

In this work, aiming at higher accuracy, we decided to use a large quantum cluster (34T) model calculated with the meta-hybrid M06-2X method that can account for those two important interactions in the zeolite framework simultaneously. The computed results compared well with the experimental measurement, especially in the case of H-ZSM-5. Therefore, we believe that the combination of models and methods presented here is appropriate for investigation of the interactions and reactions of acetone with the Brønsted acid site of zeolites.

TABLE 1: Optimized Structural Parameters of the Acetone/Zeolite Cluster Complexes in the Three Zeolites As Obtained from M06-2X/6-31G(d,p) Calculations

	H-FER				**H-ZSM-5**				H-MCM-22			
	bare	AD	TS	PR	bare	AD	TS	PR	bare	AD	TS	PR
						Distance						
Si1−O1	1.67	1.64	1.59	1.59	1.65	1.63	1.59	1.58	1.67	1.63	1.60	1.60
Si2−O2	1.58	1.57	1.64	1.66	1.59	1.57	1.62	1.64	1.60	1.59	1.64	1.65
O1−Al	1.87	1.81	1.72	1.71	1.82	1.78	1.71	1.69	1.80	1.75	1.69	1.68
O2−Al	1.67	1.67	1.79	1.82	1.68	1.69	1.77	1.80	1.67	1.68	1.76	1.77
Al ··· Hz	2.30	2.44	2.93	3.01	2.35	2.45	3.19	3.52	2.43	2.43	3.06	3.08
O1−Hz	0.97	1.10	1.74	1.83	0.97	1.11	1.80	2.08	0.97	1.16	1.90	1.94
Hz ··· O3		1.36	0.99	0.98		1.32	0.99	0.97		1.24	0.98	0.97
O1 ··· O3		2.43	2.71	2.80		2.42	2.74	2.91		2.39	2.70	2.73
O3−C1	1.21	1.23	1.32	1.34	1.21	1.23	1.31	1.33	1.21	1.24	1.31	1.32
C1−C2	1.52	1.50	1.38	1.36	1.52	1.49	1.38	1.36	1.52	1.49	1.38	1.37
C2−Ha	1.09	1.09	1.56	1.92	1.09	1.10	1.43	1.76	1.09	1.09	1.50	1.60
C1 ··· Ha	2.14	2.14	2.24	2.46	2.14	2.10	2.07	2.25	2.14	2.14	2.19	2.23
Ha ··· O2		2.36	1.14	1.02		2.67	1.20	1.04		2.81	1.14	1.09
O1 ··· O2	2.56	2.59	2.65	2.66	2.49	2.52	2.54	2.52	2.60	2.63	2.62	2.61
C1 ··· O1		3.23	3.30	3.37		3.23	3.27	3.37		3.20	3.21	3.23
C1 ··· O2		3.60	3.20	3.31		3.09	3.09	3.19		3.64	3.18	3.18
C2 ··· O2		3.33	2.67	2.89		2.99	2.63	2.79		3.03	2.63	2.68
						Angle						
Al−O1−Si1	141.8	139.5	141.5	141.1	130.6	128.4	127.6	127.4	125.0	123.5	123.4	123.2
Al−O2−Si2	150.7	153.0	146.3	146.8	133.3	135.8	133.0	133.0	124.5	125.8	126.0	126.2
O1−Hz−O3		165.8	167.1	167.8		177.6	156.8	142.0		171.7	137.3	136.1
O1−Al−O2	92.5	95.8	98.0	97.8	90.4	93.1	93.7	92.4	97.2	100.0	98.8	98.4

3.3.3. Tautomerization of Acetone on H-FER, H-ZSM-5 and H-MCM-22. The tautomerization of acetone on the Brønsted acid site of zeolite starts by the adsorption of acetone on the active site shown in Figure 4. The acetone molecule is stabilized by forming a hydrogen bond complex with the zeolite acid site. The computed adsorption energies are in the following order: −23.9, −26.9, and −28.1 for H-MCM-22, H-FER, and H-ZSM-5, respectively. These adsorption energies would suggest that the hydrogen bond between the adsorbed acetone and zeolite acid site on H-ZSM-5 is the strongest and on the H-MCM-22 is the weakest. However, when looking at the structural parameters of the optimized complex, it is observed that the hydrogen bond distance (O1···O3) in the H-MCM-22 is the shortest at 2.39 Å and the hydrogen bond angle (O1-Hz-O3) is also close to the linear angle (171.7°), indicating a very strong hydrogen bond interaction. In H-MCM-22, the adsorption causes the Brønsted O1−Hz bond distance to be significantly lengthened from 0.97 to 1.16 Å. The carbonyl double bond (O3−C1) is lengthened from 1.21 to 1.24 Å, and the C1−C2 single bond distance is decreased from 1.52 to 1.49 Å, indicating that the adsorbed acetone is activated. In H-ZSM-5, the hydrogen bond distance (O1···O3) is longer than in H-MCM-22 (2.42 Å). Therefore, the adsorbed acetone is somewhat less activated. The carbonyl double bond (O3−C1) is lengthened to 1.23 Å, and the C1−C2 single bond distance is decreased to 1.49 Å. The hydrogen bond complex in H-FER is observed to have the weakest hydrogen bond interaction. The hydrogen bond angle (O1−Hz−O3) is 165.8°, and the hydrogen bond distance (O1···O3) is 2.43 Å. The adsorbed acetone is, thus, least activated. The O3−C1 bond distance is lengthened to 1.23 Å and the C1−C2 bond distance is slightly decreased to 1.50 Å. At the transition state, the Brønsted proton is completely transferred to the carbonyl oxygen atom. For example, in the case of H-MCM-22, the O1−Hz bond elongates from 1.16 to 1.90 Å. The O3−C1 bond distance increases to 1.31 Å as the O3−Hz hydroxyl bond is formed with a bond length of 0.98 Å. The C1−C2 bond distance is reduced to 1.38 Å, indicating the double bond formation.

The activation energy of acetone tautomerization on the zeolite acid site is much smaller than in the isolated gas phase and in the water-assisted system. The zeolite acid site can greatly reduce the activation barrier. The computed activation energies are 16.6, 20.5, and 24.9 kcal/mol for the reaction in H-MCM-22, H-ZSM-5, and H-FER, respectively. The activation energies for acetone enolization in zeolites are in the same range with the free energy of activation for the reaction catalyzed by diluted mineral acid in aqueous solutions of 23.6 kcal/mol (at 298 K).[41] The activation energy trend is directly related to the strength of the hydrogen bond interactions between the adsorbed acetone and the Brønsted acid site but not to the overall adsorption interactions.

In these three representative cases, the adsorbed acetone molecule can get closer to the acid site in a geometry with larger pores and, thus, form a stronger hydrogen bonds and more activated adsorption complexes. The reaction energies for the transformation of adsorbed keto to enol of acetone are found to be 15.9, 17.6, and 22.7 kcal/mol in H-MCM-22, H-ZSM-5, and H-FER, respectively. These values are significantly higher than the reaction energy observed in diluted solutions of mineral acids (10.3 kcal/mol).[41] The higher endothermic reaction energy is due to the fact that the adsorbed acetone is highly stabilized by a strong hydrogen bond with the acid site but the produced acetone enol is weakly adsorbed on the acid site by a weak π interaction. Among these three zeolites, the difference in the energies between adsorbed acetone and acetone enol decrease with the increase of pore dimensions. However, the observed reaction energy trend is not simply due to the confinement effect of the zeolite walls. It is more likely to be related to the local interaction of the adsorbed enol form with the Brønsted acid site. The large cavity of H-MCM-22 can better accommodate the bulkier acetone enol, as reflected by a closer intermolecular distance of the C2 carbon atom of the adsorbed enol to the Ha proton of the acid site. The distances are 1.60, 1.76, and 1.92 Å for H-MCM-22, H-ZSM-5, and H-FER, respectively.

It is noticed that the structures of the transition state and the product are very similar and the reverse reaction to transform

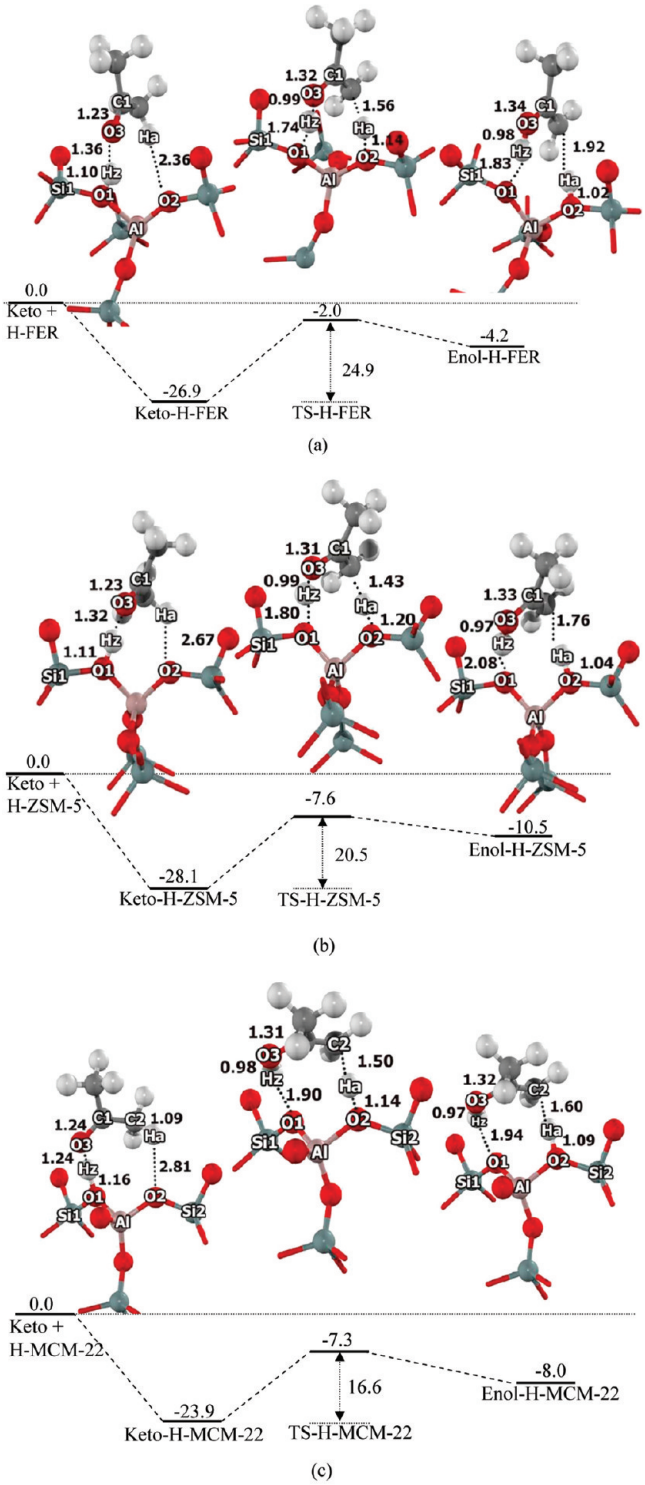

Figure 4. Molecular structures and energy profile of the tautomerization of acetone in a 34T model of (a) H-FER, (b) H-ZSM-5 and (c) H-MCM-22 as obtained from M06-2X/6-31+G(2df,2p)//M06-2X/6-31G(d,p) calculations. Distances and energies are given in Å and kcal/mol.

the adsorbed enol to the adsorbed keto form is very facile on zeolite surfaces with a small activation barrier. The activation energy of the ketonization process in these zeolites is calculated to be 0.7, 2.9, and 2.2 kcal/mol for H-MCM-22, H-ZSM-5, and H-FER, respectively, although the activation barrier for acetone ketonization in diluted mineral acid was experimentally measured to be 12.3 kcal/mol.[41] The reason for the small reverse activation energies and their trend among these three zeolites should be due to the relative stability of the adsorbed enol compared with the adsorbed acetone on the zeolite acid site. Acetone enol is much less stabilized than the adsorbed acetone on the zeolite acid site. This observation is in agreement with several experimental studies of reactions of carbonyl compounds in zeolites in which the enol form could not be detected.[4,5,45] The involvement of the enol form in carbonyl transformations was experimentally suggested by the observation of H/D exchange[45] and chlorination of acetone on the Brønsted acid site of zeolites.[5] These experimental results would indicate that the reaction of acetone would be processed through the enol form, which, however, is highly unstable in the zeolite framework. Our results clearly illustrate the relative stabilities of keto and enol forms of acetone in these three zeolites. The energies of reactants, transition states and products have also been calculated with the B3LYP functional. As expected, these adsorption energies are much smaller or there is no binding at all. Their values are given in the Supporting Information.

4. Conclusions

The effect of zeolite pore confinement on the tautomerization of acetone has been studied on three zeolites with different pore sizes. The use of a large cluster model with M06-2X/6-311+G(2df,2p)//M06-2X/6-31G(d,p) level of theory is found to be sufficient to account for interactions of acetone with the zeolite acid site and pore environments. The adsorption energies are calculated to be −26.9, −28.1, and −23.9 kcal/mol for H-FER, H-ZSM-5, and H-MCM-22, respectively, which agree well with the available experimental data for H-ZSM-5. Due to the involvement of the zeolite Brønsted acid site and the confinement effect, the tautomerization of acetone in zeolite proceeds through a much lower activation barrier than in the isolated gas phase and in the presence of water molecules. The activation energies and reaction energies decrease with the increase in the zeolite pore sizes, which are 24.9, 20.5, and 16.6 kcal/mol and 22.7, 17.6, and 15.9 kcal/mol, for the reaction in H-FER, H-ZSM-5, and H-MCM-22, respectively. The fact that the adsorption energy and activation energy trends are not correlated but rather in opposite directions indicates that the interaction with the acid site and the confinement effect of the pore walls are equally important and must be carefully accounted for to understand this reaction in zeolites. These trends are more related to the relative strength of the interactions of the active intermediates with the Brønsted acid site than to the confinement effect of the zeolite walls. The large pore of H-MCM-22 allows the adsorbed acetone and acetone enol to be closer to the acid site for stronger interactions. Therefore, both acetone enolization and (reverse) ketonization are very facile in this large-pore zeolite.

Acknowledgment. This work was supported in part by grants from the National Science and Technology Development Agency (2009 NSTDA Chair Professor funded by the Crown Property Bureau under the management of the National Science and Technology Development Agency and NANOTEC Center of Excellence funded by the National Nanotechnology Center), The Thailand Research Fund, the Commission of Higher Education, Ministry of Education ("the National Research University Project of Thailand (NRU)" and "Postgraduate Education and Research Programs in Petroleum and Petrochemicals and Advanced Materials"). Support from the Kasetsart University Research and Development Institute (KURDI) and Graduate School Kasetsart University are also acknowledged. The authors are grateful to Donald G. Truhlar and Yan Zhao

for their support with the M06-2X functional. M.P. acknowledges support from the Austrian Ministry of Science BMWF as part of the Uni-Infrastrukturprogramm of the research platform Scientific Computing at LFU Innsbruck.

Supporting Information Available: Table S1: Selected geometrical parameters for adsorption and reaction mechanism of acetone on H-FER, H-ZSM-5, and H-MCM-22 zeolites. Table S2: The adsorption and reaction energies of acetone on H-FER, H-ZSM-5, and H-MCM-22 zeolites with various methods. This material is available free of charge via the Internet at http://pubs.acs.org.

References and Notes

(1) Evans, D. A.; Nelson, J. V.; Vogel, E.; Taber, T. R. *J. Am. Chem. Soc.* **1981**, *103*, 3099.
(2) Salvapati, G. S.; Ramanamurty, K. V.; Janardanarao, M. *J. Mol. Catal.* **1989**, *54*, 9.
(3) Li, C. J. *Chem. Rev. (Washington, DC)* **1993**, *93*, 2023.
(4) Xu, T.; Munson, E. J.; Haw, J. F. *J. Am. Chem. Soc.* **1994**, *116*, 1962.
(5) Biaglow, A. I.; Sepa, J.; Gorte, R. J.; White, D. *J. Catal.* **1995**, *151*, 373.
(6) Panov, A. G.; Fripiat, J. J. *J. Catal.* **1998**, *178*, 188.
(7) Dumitriu, E.; Hulea, V.; Fechete, I.; Auroux, A.; Lacaze, J. F.; Guimon, C. *Microporous Mesoporous Mater.* **2001**, *43*, 341.
(8) Melo, L.; Giannetto, G.; Cardozo, L.; Llanos, A.; Garcia, L.; Magnoux, P.; Guisnet, M.; Alvarez, F. *Catal. Lett.* **1999**, *60*, 217.
(9) Yang, P.; Shang, Y.; Yu, J.; Wang, J.; Zhang, M.; Wu, T. *J. Mol. Catal. A: Chem.* **2007**, *272*, 75.
(10) Rodriguez-Santiago, L.; Vendrell, O.; Tejero, I.; Sodupe, M.; Bertran, J. *Chem. Phys. Lett.* **2001**, *334*, 112.
(11) Wu, C.-C.; Lien, M.-H. *J. Phys. Chem.* **1996**, *100*, 594.
(12) Lee, D.; Kim, C. K.; Lee, B.-S.; Lee, I.; Lee, B. C. *J. Comput. Chem.* **1997**, *18*, 56.
(13) Cucinotta, C. S.; Ruini, A.; Catellani, A.; Stirling, A. *ChemPhysChem* **2006**, *7*, 1229.
(14) Zakharov, M.; Masunov, A. E.; Dreuw, A. *J. Phys. Chem. A* **2008**, *112*, 10405.
(15) Solans-Monfort, X.; Bertran, J.; Branchadell, V.; Sodupe, M. *J. Phys. Chem. B* **2002**, *106*, 10220.
(16) Rattanasumrit, A.; Ruangpornvisuti, V. *J. Mol. Catal. A: Chem.* **2005**, *239*, 68.
(17) Zicovich-Wilson, C. M.; Corma, A.; Viruela, P. *J. Phys. Chem.* **1994**, *98*, 10863.
(18) Derouane, E. G. *J. Mol. Catal. A: Chem.* **1998**, *134*, 29.
(19) Derouane, E. G.; Chang, C. D. *Microporous Mesoporous Mater.* **2000**, *35*−*36*, 425.
(20) Boekfa, B.; Sirijareansre, J.; Pantu, P.; Limtrakul, J. *Stud. Surf. Sci. Catal.* **2004**, *154B*, 1582.
(21) Pantu, P.; Boekfa, B.; Limtrakul, J. *J. Mol. Catal. A: Chem.* **2007**, *277*, 171.
(22) Namuangruk, S.; Khongpracha, P.; Pantu, P.; Limtrakul, J. *J. Phys. Chem. B* **2006**, *110*, 25950.
(23) Namuangruk, S.; Pantu, P.; Limtrakul, J. *ChemPhysChem* **2005**, *6*, 1333.
(24) Boekfa, B.; Choomwattana, S.; Khongpracha, P.; Limtrakul, J. *Langmuir* **2009**, *25*, 12990.
(25) Zhao, Y.; Truhlar, D. G. *Theor. Chem. Acc.* **2008**, *120*, 215.
(26) Zhao, Y.; Truhlar, D. G. *J. Phys. Chem. C* **2008**, *112*, 6860.
(27) Maihom, T.; Boekfa, B.; Sirijaraensre, J.; Nanok, T.; Probst, M.; Limtrakul, J. *J. Phys. Chem. C* **2009**, *113*, 6654.
(28) Morris, R. E.; Weigel, S. J.; Henson, N. J.; Bull, L. M.; Janicke, M. T.; Chmelka, B. F.; Cheetham, A. K. *J. Am. Chem. Soc.* **1994**, *116*, 11849.
(29) Van Koningsveld, H.; Van Bekkum, H.; Jansen, J. C. *Acta Crystallogr., Sect. B: Struct. Sci.* **1987**, *B43*, 127.
(30) Kennedy, G. J.; Lawton, S. L.; Rubin, M. K. *J. Am. Chem. Soc.* **1994**, *116*, 11000.
(31) Nieminen, V.; Sierka, M.; Murzin, D. Y.; Sauer, J. *J. Catal.* **2005**, *231*, 393.
(32) Lonsinger, S. R.; Chakraborty, A. K.; Theodorou, D. N.; Bell, A. T. *Catal. Lett.* **1991**, *11*, 209.
(33) Zhou, D.; Bao, Y.; Yang, M.; He, N.; Yang, G. *J. Mol. Catal. A: Chem.* **2006**, *244*, 11.
(34) Schlegel, H. B. *J. Comput. Chem.* **1982**, *3*, 214.
(35) Gonzalez, C.; Bernhard Schlegel, H. *J. Chem. Phys.* **1989**, *90*, 2154.
(36) Curtiss, L. A.; Zygmunt, S. A.; Iton, L. E. *Proc. Int. Zeolite Conf.* **1999**, *1*, 415.
(37) Zygmunt, S. A.; Curtiss, L. A.; Zapol, P.; Iton, L. E. *J. Phys. Chem. B* **2000**, *104*, 1944.
(38) Frisch, M. J.; Trucks, G. W.; Schlegel, H. B.; Scuseria, G. E.; Robb, M. A.; Cheeseman, J. R.; Montgomery, J. A., Jr.; Vreven, T.; Kudin, K. N.; Burant, J. C.; Millam, J. M.; Iyengar, S. S.; Tomasi, J.; Barone, V.; Mennucci, B.; Cossi, M.; Scalmani, G.; Rega, N.; Petersson, G. A.; Nakatsuji, H.; Hada, M.; Ehara, M.; Toyota, K.; Fukuda, R.; Hasegawa, J.; Ishida, M.; Nakajima, T.; Honda, Y.; Kitao, O.; Nakai, H.; Klene, M.; Li, X.; Knox, J. E.; Hratchian, H. P.; Cross, J. B.; Adamo, C.; Jaramillo, J.; Gomperts, R.; Stratmann, R. E.; Yazyev, O.; Austin, A. J.; Cammi, R.; Pomelli, C.; Ochterski, J. W.; Ayala, P. Y.; Morokuma, K.; Voth, G. A.; Salvador, P.; Dannenberg, J. J.; Zakrzewski, V. G.; Dapprich, S.; Daniels, A. D.; Strain, M. C.; Farkas, O.; Malick, D. K.; Rabuck, A. D.; Raghavachari, K.; Foresman, J. B.; Ortiz, J. V.; Cui, Q.; Baboul, A. G.; Clifford, S.; Cioslowski, J.; Stefanov, B. B.; Liu, G.; Liashenko, A.; Piskorz, P.; Komaromi, I.; Martin, R. L.; Fox, D. J.; Keith, T.; Al-Laham, M. A.; Peng, C. Y.; Nanayakkara, A.; Challacombe, M.; Gill, P. M. W.; Johnson, B.; Chen, W.; Wong, M. W.; Gonzalez, C.; Pople, J. A. *Gaussian 03, revision B.05*; Gaussian, Inc.: Pittsburgh, PA, 2003.
(39) Holmes, J. L.; Lossing, F. P. *J. Am. Chem. Soc.* **1982**, *104*, 2648.
(40) Turecek, F.; Havlas, Z. *J. Org. Chem.* **1986**, *51*, 4066.
(41) Chiang, Y.; Kresge, A. J.; Schepp, N. P. *J. Am. Chem. Soc.* **1989**, *111*, 3977.
(42) Klinowski, J. *Chem. Rev.* **1991**, *91*, 1459.
(43) Freude, D.; Klinowski, J.; Hamdan, H. *Chem. Phys. Lett.* **1988**, *149*, 355.
(44) Sepa, J.; Lee, C.; Gorte, R. J.; White, D.; Kassab, E.; Evleth, E. M.; Jessri, H.; Allavena, M. *J. Phys. Chem.* **1996**, *100*, 18515.
(45) Xu, M.; Wang, W.; Hunger, M. *Chem. Commun. (Cambridge, U. K.)* **2003**, 722.

JP1058947